Numerical snowpack model simulation schemes for avalanche prediction in Japan

Hiroyuki HIRASHIMA[1]

1. Snow and Ice Research Center, National Research Institute for Earth Science and Disaster Resilience, Nagaoka, 940-0821, Japan

(Received November 24, 2017; Revised manuscript accepted January 25, 2019)

Abstract

This paper presents simulation schemes, developed by National Research Institute for Earth Science and Disaster Resilience (NIED), for stability indices and liquid water infiltration that may be applied to a range of numerical snowpack models for avalanche prediction. The schemes were originally developed in the SNOWPACK model, and are introduced for wider application using flow charts, equations, and parameter tables for simulation of the natural stability index, shear strength, and water content. Validation of the stability indices was performed through simulations of eight recent surface avalanche accidents. Even though the simulations did not explicitly consider the weak layer formed by brittle precipitation particles that triggered most of the recent avalanches, they show that avalanche risks are high when stability indices are below a threshold of 2. This result supports previous work and demonstrates the wider applicability of the schemes for providing information on snowpack stability. However, estimation of avalanche risk could be improved through incorporation of information on snow crystal type and associated metamorphism parameterization in numerical snowpack models.

Keywords: numerical snowpack model, avalanche prediction, liquid water movement, shear strength

1 Introduction

Avalanche forecasting using the numerical snowpack model SNOWPACK is performed as part of the snow disaster forecasting project of the Snow and Ice Research Center (SIRC), National Research Institute for Earth Science and Disaster Resilience (NIED), Japan (Nakai *et al.*, 2012). The SNOWPACK model was initially developed by Bartelt and Lehning (2002) and Lehning *et al.* (2002a, b) for avalanche forecasting in Switzerland and was first applied in Japan by Hirashima *et al.* (2004) and Yamaguchi *et al.* (2004). Since then, the model has been adapted and improved to enhance the accuracy of avalanche detection in Japan. The main improvements to the model involve the use of a new parameter for shear strength estimation, the dry snow metamorphism factor (Hirashima *et al.*, 2009, 2011), and the incorporation of water transport processes through layered snow (Hirashima *et al.*, 2010). Validation of the SNOWPACK model using snow pit observation data for snow temperature, density, water content, and grain size is reported in Hirashima *et al.* (2015), and the improvements are reviewed in Hirashima (2014).

The SNOWPACK model is applied to estimate avalanche risk using the stability index. A stability index of 1.5 or below is usually taken as the threshold for avalanche risk (Sommerfeld, 1984). However, in applications of the SNOWPACK model to specific avalanches in Japan (Nishimura *et al.*, 2005; Sato *et al.*, 2007; Hirashima *et al.*, 2006, 2008; Takeuchi *et al.*, 2011; Takeuchi and Hirashima 2013; Abe and Hirashima 2015), many avalanches occurred when the simulated stability index was 2 or below. Therefore, Hirashima *et al.* (2006, 2008) suggested that a stability index threshold of 2 was more appropriate for evaluating avalanche susceptibility in Japan.

This paper presents prediction schemes that allow the stability index algorithms to be implemented in other numerical snowpack models in Japan (e.g., Niwano *et al.*, 2012). Although many descriptions of the SNOWPACK parameterized in Japan are noted in the review of Hirashima (2014), they focused on successful improvements of SNOWPACK in Japan. In contrast, this paper focuses on procedures for applying the simulation to other numerical snowpack models, including how to obtain input data from meteorological observations (Hirashima *et al.*, 2008), and from equations and flow charts for the calculation of shear strength, and liquid water movement. Simulated stability indices for recent avalanches are also discussed in the context of model validation.

2 Procedure for snowpack simulation and avalanche prediction

2.1 Preparation of input data for snowpack simulation

The SNOWPACK model is the main core of the avalanche prediction system, a component of the Snow Disaster Forecasting System (Nakai *et al.*, 2012). Input data for SNOWPACK are derived from meteorological observation data, mainly obtained from the SIRC and the Japanese Meteorological Agency (JMA). The JMA has 1311 Automated Meteorological Data Acquisition System (AMeDAS) stations and 60 local meteorological observatory stations.

Meteorological data observed with AMeDAS include air temperature, wind speed, wind direction, sunshine duration, precipitation, and snow depth. The SNOWPACK model requires inputs of air temperature, relative humidity, wind speed, wind direction, solar radiation, longwave radiation, precipitation, and snow depth. Additional information, such as height of instruments, are written in the initial setup file, which has a file extension of '.ini'. The height of instruments affects bulk coefficients to calculate sensible and latent heat fluxes. Although some of the input data may be directly taken from observations, some parameters must be estimated indirectly. If snow depth data are available at a JMA meteorological station close to the simulated location, snowfall amount is estimated from snow depth. However, owing to high spatial variation in snow depth with elevation and orientation, precipitation is usually used to derive snow depth at the avalanche slope. Input air temperature is corrected using an elevational lapse rate of 0.0065 $^{\circ}C\ m^{-1}$.

The AMeDAS data does not include solar and downward longwave radiations, which significantly influence snowmelt amount and snow temperature, and are required inputs to the model; these must be estimated from other meteorological parameters. First, the solar radiation for ground with zero tilt is estimated based on the equations of Kondo *et al.* (1991), as reported in Kondo (1994) using sunshine duration, air temperature, longitude, latitude, date and time. This estimation neglects the effect of surrounding terrain such as shadow, reflection of back scattering, and downward longwave radiation received from the snow or ground surface. First, the whole solar radiation is calculated by the equation of Kondo *et al.* (1991) and then it is classified into direct solar radiation and diffuse solar radiation. The ratio of direct solar radiation to whole solar radiation is assumed to be equal to the ratio of sunshine duration to possible sunshine duration. The diffuse solar radiation is derived form the difference between whole solar radiation and direct solar radiation. Direct solar radiation is corrected using slope angle, slope direction, solar angle, and solar direction. Downward longwave radiation is also estimated based on the equation of Kondo *et al.* (1991). If meteorological data provided by other agencies (e.g., Ministry of Land, Infrastructure, Transport and Tourism, or local government) are available for sites closer to the avalanche slope, that data is substituted. The meteorological data collected by other agencies usually includes air temperature, precipitation, or snow depth.

The Japan Meteorological Agency Non-Hydrostatic Model (JMANHM; Saito *et al.*, 2006), which has a resolution of 1.5 km operated by NIED, is used to provide 30-hour-long meteorological forecast data beginning at 09 and 21 UTC daily. The JMANHM outputs for 0–20 m elevation provide all of the meteorological parameters necessary for input into the SNOWPACK model.

To perform real-time simulations for several avalanche slopes, a prediction table is prepared in advance (Table 1). Observed and forecasted meteorological data are connected to make the input data. Simulation is updated for every three hours replacing forecasted data with latest observed data (Fig. 1). The duration of each simulation is from the beginning of winter (usually December 1 in Honshu island) to the last time of forecasted meteorological data. The SNOWPACK simulation is completed within 20 min for the whole winter at one location in single core simulations. We presently use Mac Pro 2012 computer with 2.4GHz, 12 core and 24 thread in Xeon CPU. Therefore, simulations for 24 slopes can be performed simultaneously every 20 minutes. Simulations for whole avalanche slopes (about 100) are completed in 2 hours. Simulated results were provided to registered users experimentally such as local governments and road administrators (Nakai *et al.*, 2012). Prediction simulations were performed and updated every 3 hours for the winter of 2016–2017.

Table1

Fig.1

2.2 Interpretation of simulations results

Although the skier stability index is used to estimate avalanche risk in Switzerland (e.g., Scheweizer *et al.*, 2006; Shirmer *et al.*, 2009), the natural stability index is used for natural avalanche prediction in Japan. The skier stability index includes the effect of the difference between snow layers for hardness and grain sizes. If the difference of hardness or grain size is large, the skier stability index is corrected to be small. The natural stability index is calculated as the ratio of shear strength to shear stress, as described in section 3. Although avalanche risk is basically estimated using stability index, the cause of instability is estimated by other information. Therefore, following information had better be considered for final decision. Information on grain type is used to estimate the cause of weak layer formation (e.g., timing of faceted crystals formation). Furthermore, information on the water content and discharge amount are required to estimate the wet snow avalanche risk. These data are included for the operation of avalanche prediction.

Figure 2 shows examples of snowpack conditions with low stability. Figure 2a is the case for unstable conditions due to heavy snowfall. Fresh snow consolidates quickly after snowfall

Fig.2

and usually strengthens enough to support newly fallen snow. However, if heavy snowfall continued for several hours, the snow is strongly loaded with newer snow before densification. In this case, snow becomes unstable even if there is no weak layer (Endo, 1992). After snowfall stops, the stability index increases rapidly. In another case (Fig. 2b), the red line at about 200 cm above the ground surface indicates a weak layer (e.g., faceted crystals). This unstable condition continues for two days after cessation of snowfall. The main control schemes used to determine the stability index in SNOWPACK are the initial density of snow (Hirashima *et al.*, 2015), compressive viscosity (Lehning *et al.*, 2002a), and the relationship of snow density and shear strength (Lehning *et al.*, 2004; Hirashima *et al.*, 2009, 2011). Note that these references are just referred written with model description. Concepts and theory were written in other previous papers.

In the present SNOWPACK model, it is difficult to estimate the wet snow full depth avalanche risk from the natural stability index (Hirashima *et al.*, 2006), and information on liquid water infiltration is used as an alternative method. When the SNOWPACK model used a bucket scheme for liquid water infiltration, the discharge amount was used as the risk index for a wet snow full depth avalanche (Hirashima *et al.*, 2006). The most recent version of the SNOWPACK model (from 2010) uses the Darcy-Buckingham law to simulate liquid water infiltration (Hirashima *et al.* 2010; Wever *et al.*, 2014). Using these schemes, a parameter calculated from volumetric liquid water content provides an estimate of wet snow avalanche risk. Figure 2c shows an increase in water content during water percolation, which leads to increased wet snow avalanche risk. Mitterer *et al.* (2013) have also developed a quantitative index to estimate wet snow avalanche risk in Switzerland. Schemes for liquid water infiltration are further described in section 4.

3 Natural stability index estimation using a dry snow metamorphism factor

The natural stability index is calculated from shear strength divided by shear stress, and was originally implemented in SNOWPACK by Lehning *et al.* (2004). In the original, equations parameterized by Jamieson and Johnston (2001), which measured at the weak layer, were used to estimate shear strength. When they were applied to heavy snowfall area in Japan, most of the snow was simulated as unstable (Hirashima *et al.*, 2008). Therefore, in Japan, the method used to estimate shear strength was modified, based on observation and laboratory experiment results (Yamanoi and Endo, 2002; Abe *et al.*, 2007), and on a new parameter, the dry snow metamorphism (DSM) factor (Hirashima *et al.*, 2009, 2011). Figure 3 shows the Fig.3

Table2

Fig.2

scheme used to estimate the DSM factor, shear strength, and the natural stability index (SI); the associated equations and parameters are explained in tables 2 and 3. The SI is calculated using Eq. (1) at all model layers, and the minimum value of SI from the entire snowpack is used as the SI for the snowpack. The shear strength used in Eq. (1) is calculated using Eq. (2), (3), and (4).

The DSM factor is one of the independent parameters and is used to estimate shear strength in Eq. (2). The initial value of the DSM factor for new snow is set to zero (Fig. 3), and it then fluctuates within the range 0 to 1. When the temperature gradient is greater than 5 ℃m^{-1}, the DSM factor increases as temperature gradient metamorphism with Eq. (5) to (10). The equations are described in detail in Hirashima *et al.* (2009). When the temperature gradient is below 5 ℃m^{-1}, the DSM factor decreases as equi-temperature metamorphism with Eq. (11) or (12). A detailed description of Eq. (11) is given in Hirashima *et al.* (2011), where the parameter was determined by linear regression based on laboratory experiments performed in the cold room at −5 ℃ and −10 ℃. Following that work, Hirashima and Abe (2012) extended the laboratory experiments to temperature conditions of −2 ℃ and −15 ℃. The results showed a positive correlation between decreasing rate of DSM factor and snow temperature at snow temperatures of lower than −5 ℃ and a negative correlation at snow

Fig.4

Fig.3

temperatures higher than −5 ℃ (Fig. 4). Based on these findings, two different equations (Eq. 11 and 12) are used depending on snow temperature. The calculated value of dC/dt is used to add or subtract the DSM factor, C. If the value of C is outside the range 0 to 1, it is corrected to 0 or 1. The new DSM factor that is calculated is used for estimation of shear strength and the next time step simulation (Fig. 3).

4 Simulation schemes for liquid water infiltration

Liquid water infiltration is simulated by the Richards equation (Richards, 1931). Liquid water fluctuation is calculated by conservation of mass (Eq. 13), and water flux is estimated by the Darcy‐Buckingham law (Eq. 14). In the snowpack, the time scale of water transport is small compared with consolidation, heat transfer, and metamorphism. In the old version of SNOWPACK (i.e., that using a bucket scheme), the time step was usually 15 min. When the same time step was used for the water transport scheme with Eq. (13) and (14), the simulation diverged. When an explicit scheme was used, the simulation diverged even if the time step was as small as 0.01 s. Although the implicit scheme permits a larger time step to be used, the residual water content and complicated processes in the SNOWPACK model make it difficult to perform a stable simulation. Hirashima *et al.* (2010) developed a technique to perform a stable simulation with relatively large time steps using explicit schemes. In the present SNOWPACK model, Wever *et al.* (2014) successfully stabilized the simulation by implementing Richard's equation with an implicit scheme and pragmatic strategy. The advantage of the technique of Hirashima *et al.* (2010) is that it is relatively easy to perform a stable simulation for more complex situation such as three-dimensional water transport (Hirashima *et al.*, 2014). Thus, this study adopted the technique of Hirashima *et al.* (2010).

The flowchart for the liquid water infiltration scheme is shown in Figure 5. Equations and parameters are defined in tables 2 and 3, respectively. When liquid water is supplied by rain or snowmelt, the liquid water content of the topmost model layer is increased following Eq. (15). Solar radiation-induced snowmelt amount at an internal layer percolated into the snowpack is also calculated using same equation. To calculate water movement, suction was estimated using the van Genuchten model (van Genuchten, 1980) with Eq. (16) and (17). Parameters for saturated and residual water content were determined based on the results of Yamaguchi *et al.* (2010) and are shown in Table 3. Parameters for the van Genuchten model were determined using Eq. (18) and (19). Hydraulic conductivity for all elements was calculated using Eq. (20), (21), and (22).

Fig.5

Usually, the water transport amount is calculated by multiplying water flux by the time step. However, as discussed, the time step must be very small if the explicit scheme is used. In the technique of Hirashima *et al.* (2010), the water transport amount for one time step is calculated using Eq. (23). Here, the water transport amount was calculated as a function of initial water flux and limitation to water transport amount, q_{lim}, to avoid divergence. The initial water flux was calculated using the Darcy–Buckingham law, Eq. (14). The parameter q_{lim} represents the water transport amount needed for equilibrium conditions between two elements and was calculated using Eq. (24). Using these equations, water transport simulations could be performed with a time step of 20 s. The detailed derivation of the equations is given in Hirashima *et al.* (2010).

A problem of this scheme is that there is too much ponding at the capillary barrier owing to the neglect of preferential flow. To avoid this problem, an upper limit of water content at the capillary barrier was set to 7%. If volumetric water content at the capillary barrier exceeds 7%, the extra water is forced to move to a lower element. The value of 7% was determined using a sensitivity experiment to estimate the optimal value to match observed snow discharge lysimeter data at the field site at SIRC, Nagaoka.

5. Estimation of the stability index for recent slab avalanches

SNOWPACK simulation results and avalanche release data have been compared in a number of previous studies (Hirashima *et al.*, 2006, 2007, 2008; Sato *et al.*, 2007; Takeuchi and Hirashima, 2013; Abe and Hirashima, 2015). Most recently, Abe and Hirashima (2015) estimated stability indices for slab avalanches induced by faceted crystal layer collapse and showed that the SNOWPACK model could successfully reproduce destabilization. Since that work, SIRC has surveyed 11 avalanches, 8 of which were surface avalanches (as listed in Table 4). The survey results are described in detail on the SIRC website (http://www.bosai.go.jp/seppyo/kenkyu_naiyou/seppyousaigai/seppyousaigai.htm). Most of the surveyed avalanches were not triggered by collapse of a faceted crystal layer, but through collapse of brittle precipitation particles.

Table4

The SNOWPACK model cannot reproduce the effect of precipitation particle type because it is not included as input data. Nevertheless, we attempted to estimate stability indices for such avalanches to validate the model simulations for this type of avalanche. Simulations were performed using the method shown in section 2, with meteorological observations obtained from the nearest AMeDAS station used for input data.

Temporal changes in the simulated SI for surface avalanche profiles are shown in Figure 6, and the SI value at the time of avalanche release is given in Table 4. In these simulations, seven of the eight avalanches have a SI at release of 2 or below, and five are below 1.5 (see Table 4). In the case of Hachimantai, in which the simulated stability index was 2.4 (Fig. 6e), the avalanche was earthquake induced and may not have been released without the earthquake trigger. Therefore, the model could estimate avalanche risk using a threshold value of 2.

Fig.6

However, as mentioned above, six of the eight avalanches were due to collapse of a weak layer formed by brittle precipitation particles. As the SNOWPACK model does not use information on the crystal type of precipitation particles, the destabilization mechanism was incorrect. Nevertheless, the simulated SI did manage to reproduce unstable conditions. Most of the simulation results showed that the layer representing the surface prior to snowfall became a weak layer (see Figs. 6 a–d, f, and h). Before snowfall, the snow surface layer would have been exposed to cold air and radiative cooling, which leads to temperature gradient metamorphism and the creation of faceted crystals. When faceted crystals are buried by subsequent snowfall, they form a weak layer. However, in many cases, survey results showed the weak layer comprised non-rimed precipitation particles rather than faceted crystals. Non-rimed snow crystals are associated with the south-coast cyclone, and snow stability decreases during large amounts of snowfall under such conditions (Ishizaka *et al.*, 2015). If there is sustained fine weather before snowfall, a weak layer of faceted crystals may also develop. In many of the avalanches, faceted crystals formed in the simulation. Consequently, the timing of snow destabilization was detected regardless of the position of the weak layer, even though the mechanism was incorrect. In these cases, days with zero precipitation were continued for more than 3 days before the south-coast cyclone approached. Furthermore, on one of these days, the sunshine duration was almost equal to possible sunshine duration, indicating that it was sunny day. Radiation cooling on sunny days led to the formation of faceted crystals at the surface in the simulation. The analysis of more cases is necessary to determine whether this trend is typical before the approach of a south-coast cyclone or not. If this trend is typical, this type of avalanche can be predicted indirectly by SNOWPACK. Nevertheless, for accurate avalanche prediction, the SNOWPACK model needs to be modified to consider precipitation particle type, with appropriate input data. The validation work also suggests that the model overestimates the formation of faceted crystals. Improvement of these elements would allow more accurate estimation of stability indices, avoidance of false alerts, and determination of stabilization after snowfall cessation.

6. Summary

This paper describes simulation schemes for providing the stability index and liquid water condition of a snowpack for avalanche prediction in Japan. These schemes are implemented in the SNOWPACK model, which uses an original parameter for shear strength (the DSM factor); this parameter is key to the improvement of avalanche risk prediction. This paper has been written to enable application of the schemes to other numerical snowpack models. Equations, parameters, and flow charts are provided to aid understanding of the simulations. Estimated stability indices have been compared with avalanche observations from several previous studies. Here, stability indices were simulated for eight recent surface avalanches. Despite most of the recent avalanches being induced by brittle precipitation particles, which are not considered by the present version of SNOWPACK, the simulated stability indices did reproduce unstable conditions. Although the existing model provides useful information for estimating avalanche risk, it needs further improvement for accurate reproduction. Implementation of information on the type of snow crystal comprising precipitation particles, and parameterization of metamorphism depending on snow crystal type, will enable more accurate estimation of avalanche risk.

Acknowledgments

This study is part of the National Research Institute for Earth Science and Disaster Resilience (NIED) project, ‘Research on Advanced Snow Information and its application to Disaster Mitigation’. I am grateful to members of the Snow and Ice Research Center for their advice and discussion. Most of schemes introduced in this paper are based on experiments performed by O. Abe and S. Yamaguchi. We are grateful to M. Miura, who assisted with our research.

References

Abe, O., Mochizuki, S., Hirashima, H. and Sato, A. (2007): Parameterization of shear strength of Faceted Snow Layers (in Japanese). *Cold Region Technology Conference*, **23**, 125-129.

Abe, O. and Hirashima, H. (2015): Evaluation of an avalanche forecasting system based on the development process of faceted crystals (in Japanese with English abstract). *J. Jpn. Soc. Snow and Ice (Seppyo)*, **77**, 37-45.

Bartelt, P. and Lehning, M. (2002): A physical SNOWPACK model for the Swiss avalanche warning. Part I: numerical model. *Cold Reg. Sci. Technol*., **35** (3), 123-145.

Calonne, N., Geindreau, C., Flin, F., Morin, S., Lesaffre, B., Rolland du Roscoat, S. and Charrier, P. (2012): 3-D image-based numerical computations of snow permeability: links to specific surface area, density, and microstructural anisotropy. *The Cryosphere*, **6**, 939-951.

Endo, Y. (1992): Time variation of stability index in new snow on slopes. *Proceedings of the Japan-U.S. workshop on snow avalanche, land-slide, debris flow prediction and control, 1991, Tsukuba, sponsored by Science and Technology Agency of Japanese Government*, 85-94.

Hirashima, H., Nishimura, K., Baba E., Hachikubo, A. and Lehning, M. (2004): SNOWPACK model simulations for snow in Hokkaido, Japan. *Ann. Glaciol.*, **38**, 123-129.

Hirashima, H., Nishimura, K., Yamaguchi, S., Sato, A. and Lehning, M. (2006): Evaluation of snow stability index in a snow cover model for avalanche accidents (in Japanese). *Cold Region Technology Conference*, **22**, 26-30.

Hirashima, H., kamiisi, I., sato, A., Matuura, T., Machida, T. and Lehning, M. (2007): Effect of meteorological input data in the accuracy of avalanche prediction -validation on the Route 17- (in Japanese). *Cold Region Technology Conference*, **23**, 192-197.

Hirashima, H., Nishimura, K., Yamaguchi, S., Sato, A. and Lehning, M. (2008): Avalanche forecasting in a heavy snowfall area using the snowpack model. *Cold Reg. Sci. Technol.*, **51** (2–3), 191-203.

Hirashima, H., Abe, O., Sato, A. and Lehning, M. (2009): An adjustme nt for kinetic growth metamorphism to improve shear strength parameterization in the SNOWPACK model. *Cold Reg. Sci. Technol.*, **59** (2–3), 169-177.

Hirashima, H., Yamaguchi, S., Sato, A. and Lehning, M. (2010): Numerical modeling of liquid water movement through layered snow based on new measurements of the water retention curve. *Cold Reg. Sci. Technol.*, **64**, 94-103.

Hirashima, H., Abe, O. and Sato, A. (2011): Parameterization of the shear strength of faceted crystals during equi-temperature metamorphism. *Ann. Glaciol.*, **52**, 111-118.

Hirashima, H. and Abe, O. (2012): Snow temperature dependency of shear strength change for faceted crystals during equi-temperature metamorphism (in Japanese). *Seppyo hokushinetsu*, **32**, 15.

Hirashima, H. (2014): Success and challenges of avalanche prediction using numerical snowpack model (in Japanese). *J. Jpn. Soc. Snow and Ice (Seppyo)*, **76**, 411-419.

Hirashima, H., Yamaguchi, S. and Katsushima, T. (2014): A multi-dimensional water transport model to reproduce preferential flow in the snowpack, *Cold Reg. Sci. Technol*., **108**, 80-90. doi: 10.1016/j.coldregions.2014.09.004.

Hirashima, H., Yamaguchi, S., Kosugi, K., Nemoto, M., Aoki, T. and Matoba, S. (2015): Validation of the SNOWPACK model using snow pit observation data (in Japanese with English abstract). *J. Jpn. Soc. Snow and Ice (Seppyo)*, **77**, 5-16.

Ishizaka, M., Fujino, T., Motoyoshi, H., Nakai, S., Nakamura, K., Shiina, T. and Muramoto, K. (2015): Characteristics of snowfalls and snow crystals caused by two extratropical cyclones passing along the Pacific Ocean side of Japan on February 8 and 14-15 observed in Niigata district, 2014 – in relation to frequent occurrence of avalanches in Kanto-Koshin areas – (in Japanese with English abstract). *J. Jpn. Soc. Snow and Ice (Seppyo)*, **77**, 285-302.

Jamieson, B. and Johnston, C. D. (2001): Evaluation of the shear frame test for weak snowpack layers. *Ann. Glaciol.*, **32**, 59-69.

Kondo, J. (1994): Mizu Kankyo no Kishogaku (Meteorology of Water Environment), Asakura-Shoten, 348pp.

Kondo, J., Nakamura, T. and Yamazaki, T. (1991): Estimation of the solar and downward atmospheric radiation (in Japanese). *Tenki*, **38**, 41-48 .

Lehning, M., Bartelt, P., Brown, B., Fierz, C. and Satyawali, P. (2002a): A physical SNOWPACK model for the Swiss avalanche warning Part II. Snow microstructure. *Cold Reg. Sci. Technol.*, **35**, 147-167.

Lehning, M., Bartelt, P., Brown, B. and Fierz, C. (2002b): A physical SNOWPACK model for the Swiss avalanche warning Part III: meteorological forcing, thin layer formation and evaluation. *Cold Reg. Sci. Technol.*, **35**, 169-184.

Lehning, M., Fierz, C., Brown, B. and Jamieson, B. (2004): Modeling snow instability with the snow-cover model SNOWPACK. *Ann. Glaciol.*, **38**, 331-338.

Mitterer, C., Techel, F., Fierz, C. and Schweizer, J. (2013): An operational supporting tool for assessing wet-snow avalanche danger. *Proceedings of International Snow Science Workshop Grenoble, Francem 7-11 October 2013. ANENA, IRSTEA, Météo-France, Grenoble, France,* 334-338.

Nakai, S., Sato, T., Sato, A., Hirashima, H., Nemoto, M., Motoyoshi, H., Iwamoto, K., Misumi, R., Kamiishi, I., Kobayashi, T., Kosugi, K., Yamaguchi, S., Abe, O. and Ishizaka, M. (2012): A Snow Disaster Forecasting System (SDFS) constructed from field observations and laboratory experiments. *Cold Reg. Sci. Technol.*, **70**, 53-61.

Nishimura, K., Baba, E., Hirashima, H. and Lehning, M. (2005): Application of the snow cover model SNOWPACK to snow avalanche warning in Niseko, Japan. *Cold Reg. Sci. Technol.*, **43**, 62-70.

Niwano, M., Aoki, T., Kuchiki, K., Hosaka, M. and Kodama, Y. (2012): Snow Metamorphism and Albedo Process (SMAP) model for climate studies: Model validation using meteorological and snow impurity data measured at Sapporo, Japan. *J. Geophys. Res.*, **117**, F03008, doi:10.1029/2011JF002239.

Richards, L. (1931): Capillary conduction of liquids through porous mediums, *J. Appl. Phys.*, **1**, 318-333, doi:10.1063/1.1745010.

Roch, A. (1966). Les Variations de la résistance de la neige. *IAHS Publication*, **69**, 86-99.

Sato, T., Hirashima, H., Nemoto. M., Mochizuki, S., Abe, O., Lehning, M., Sato, A., Hanaoka, M., Akiyama, K., Murakami, S. and Daimaru, H. (2007): Slab avalanches occurred at Tsurunoyu in Nyuutou Onsen, Akita Prefecture, Japan (in Japanese with English Abstract). *J. Jpn. Soc. Snow and Ice (Seppyo)*, **69**, 445-456.

Saito, K., Fujita, T., Yamada, Y., Ishida, J., Kumagai, Y., Aranami, K., Ohmori, S., Nagasawa, R., Kumagai, S., Muroi, C., Kato, T., Eito, H., and Yamazaki, Y. (2006): The operational JMA nonhydrostatic mesoscale model. *Mon. Wea. Rev.*, **134**, 1266-1298.

Schweizer, J., Bellaire, S., Fierz, C., Lehning, M. and Pielmeier, C. (2006): Evaluating and improving the stability predictions of the snow cover model SNOWPACK. *Cold Reg. Sci. Technol.*, **46**(1), 52-59.

Schirmer, M., Lehning, M. and Schweizer, J. (2009): Statistical forecasting of regional avalanche danger using simulated snow-cover data. *J. Glaciol.*, **55**, 761-768.

Sommerfeld, R.A. (1984): Instructions for using the 250 cm^2 shear frame to evaluate the strength of a buried snow surface. *U.S. For. Serv. Res. N*ote *RM-446*, 1-6.

Takeuchi, Y., Torita, H., Nishimura, K. and Hirashima, H. (2011): Study of a large-scale dry slab avalanche and the extent of damage to a cedar forest in the Makunosawa valley, Myoko, Japan. *Ann. Glaciol.*, **52**(58), 119-128.

Takeuchi, Y. and Hirashima, H. (2013): Snowpack estimations in the starting zone of large-scale snow avalanches in the Makunosawa valley, Myoko, Japan. *Ann. Glaciol.*, **54**(62), 19-24.

van Genuchten, M. T. (1980): A closed-form equation for predicting the hydraulic conductivity of unsaturated soils. *Soil Sci. Soc. Am. J.*, **44**(6), 892-898.

Wever, N., Fierz, C., Hirashima, H. and Lehning, M. (2014): Solving Richards Equation for snow improves snowpack meltwater runoff estimations in detailed multi-layer snowpack model. *The Cryosphere*, **8**, 257-274.

Yamaguchi, S., Sato, A. and Lehning, M. (2004): Application of the numerical snowpack model (SNOWPACK) to the wet-snow region in Japan. *Ann. Glaciol.*, **38**, 266-272.

Yamaguchi, S., Katsushima, T., Sato, A. and Kumakura, T. (2010): Water retention curve of snow with different grain sizes. *Cold Reg. Sci. Technol*., **64**(2), 87-93.

Yamaguchi, S., Watanabe, K., Katsushima, T., Sato, A. and Kumakura, T. (2012): Dependence of the water retention curve of snow on snow characteristics. *Ann. Glaciol.*, **53**(61), 6-12.

Yamanoi, K. and Endo, Y. (2002): Dependence of shear strength of snow cover on density and water content (in Japanese with English abstract). *J. Jpn. Soc. Snow and Ice (Seppyo)*, **64**, 443-451.

List of Tables

Figure Captions

Figure 1 Schedule to update snowpack information. Yellow: using observed data; green: using predicted data. Meteorological prediction data is updated for every 12 hours.

Figure 2 Examples of low stability snowpacks at risk of avalanche under; a: heavy snowfall, b: snowfall with a weak layer, and c: wet snow with liquid water infiltration.

Figure 3 Flow chart for simulation of the natural stability index using DSM factor to estimate avalanche risk. See Table 3 for explanation of symbols.

Figure 4 Rate of reduction of the dry snow metamorphism (DSM) factor during equi-temperature metamorphism depending on snow temperature (Hirashima *et al.*, 2011; Hirashima and Abe, 2012).

Figure 5 Flow chart for simulation of liquid water infiltration into the snowpack. See Table 3 for explanation of symbols.

Figure 6 Simulated natural stability indices for surface avalanches in 2014–2017. Red arrows show the timings of avalanche release. See Table 4 for details of the avalanches.

Table 1 Example of an input data record for estimating avalanche risk for specific avalanche slopes

Name	Latitude	Latitude_min	Latitude_sec	Longitude	Longitude_min	Longitutde_sec	Altitude	Slope Angle	Slope Direction	JMA data	other data	Eng_Name
								0	WNW	高田（Takada）		

Table 2 Equations used in schemes to simulate the natural stability index (Eq. 1–12) and liquid water infiltration (Eq. 13–24). See Table 3 for explanation of parameters

Equation	Parameter	Reference
	$\overline{gh_d \sin\varphi \cos\varphi}$	
	$h = \frac{1}{a}\left(\theta^{-\frac{1}{m}} - 1\right)^{\frac{1}{n}}$	

Table 3 Parameters used in the equations shown in Table 2

Symbol	Parameter	Value	Unit
Δt	One time step		s
Δz_1	Thickness of element for upper layer		m
Δz_2	Thickness of element for lower layer		m
a	Parameter for water retention curve		m^{-1}
C	Dry snow metamorphism factor	0 to 1	-
d	Grain diameter		mm
D_0	Water vapor diffusion coefficient at 0 ℃ and 1 atm	2.23×10^{-5}	m^2s^{-1}
D_{air}	Water vapor diffusion coefficient in atmosphere	Eq. 8	m^2s^{-1}
D_{eff}	Empirical equation of diffusion coefficient in snowpack	Eq. 9	m^2s^{-1}
D_{snow}	Water vapor diffusion coefficient in snow	Eq. 7	m^2s^{-1}
g	Acceleration due to gravity	9.8	ms^{-2}
$h(\theta)$	Suction at volumetric water content, θ	Eq. 16	m
h_d	Vertical thickness of snow from target snow		m
K	Hydraulic conductivity	Eq. 22	ms^{-1}
K_r	Relative hydraulic conductivity	Eq. 21	-
K_s	Saturated hydraulic conductivity	Eq. 20	ms^{-1}
L	Latent heat of sublimation	2.838×10^6	Jkg^{-1}
n	Parameter for water retention curve		-
$q\Delta t$	Water transport amount in one time step	Eq. 23	m
q_0	Water flux in Darcy–Backingham law	Eq. 14	ms^{-1}
q_{lim}	Water transport amount for equilibrium condition between two elements	Eq. 24	ms^{-1}
R_v	Gas constant for water vapor	461.9	$m^2s^{-2}K^{-1}$
S	Shear strength	Eq. 2	Pa
S_{DH}	Shear strength of depth hoar	Eq. 4	Pa
SI	Natural stability index	Eq. 1	-
S_{RG}	Shear strength of rounded grains	Eq. 3	kPa
t	Time		s
T_0	Triple point temperature	0.01	℃
T_a	Air temperature		℃
T_s	Snow temperature		℃
z	Snow height		m
α	Coefficient reflecting a DSM factor increment	Eq. 6	m^2kg^{-1}
θ	Volumetric water content		-
Θ	Effective water saturation	Eq. 17	-
θ_1	Volumetric water content for upper layer		-
θ_2	Volumetric water content for lower layer		-
θ_r	Residual water content	0.024	-
θ_s	Saturated water content	0.9 × porosity	-
ν	Kinematic viscosity coefficient of water at 0 ℃	1.792×10^{-3}	m^2s^{-1}
ρ	Snow density		kgm^{-3}
ρ_0	Triple point pressure	610.6	Pa
ρ_v	Saturated water vapor pressure	Eq. 10	Pa
φ	Slope angle		degree

Table 4 Details of avalanches used for validation in this study. The letters a–h refer to the stability index simulations shown in Figure 5

Figure	Place	Time	overview and damege	victim	weak layer	Location	elevation (m)	slope direction	meteorological data	simulated SI
a	Sekiyama-touge	2014/2/15 12:00	Two cars were involved, no injury.	0	brittle snow crystal type	38° 23' 72" N 140° 33' 59" E	850	W	Murayama	1.3
b	Sekiyama-touge	2015/1/31 23:35	Cars were stranded	0	brittle snow crystal type	38° 23' 72" N 140° 33' 59" E	850	W	Murayama	1
c	Kannon-tera	2015/1/31 23:05	Cars were stranded	0	brittle snow crystal type	38° 25' 33" N 140° 31' 53" E	483	N	Murayama	1
d	Nishikawa-cho	2015/2/11 19:35	A car was involved, no injury	0	brittle snow crystal type	38° 21' 49" N 139° 55' 2" E	730	WSW	Ooisawa	1.9
e	Hachimantai	2015/2/17 8:06	Induced by earthquake. No injuried	0	faceted crystals	39° 58' 34" N 140° 48' 8" E	1110	E	Iwatematsuo	2.4
f	Maehotaka	2016/1/31 11:45	A man was involved and died after rescued	1	brittle snow crystal type	36° 47' 25" N 139° 8' 46" E	1930	NE	Fujiwara	1
g	Togarionsen	2017/2/13 8:10	Three people were involved and one person was died	1	FF on melt forms	36° 55' 38" N 138° 23' 3" E	930	ESE	Nozawaonsen	2
h	Nasu	2017/3/27 8:30	More than 40 people were involved and eight people were died, 38 people were injuried.	8	brittle snow crystal type	31° 7' 6" N 139°59' 5" E	1350	E	Nasukougen	1.1

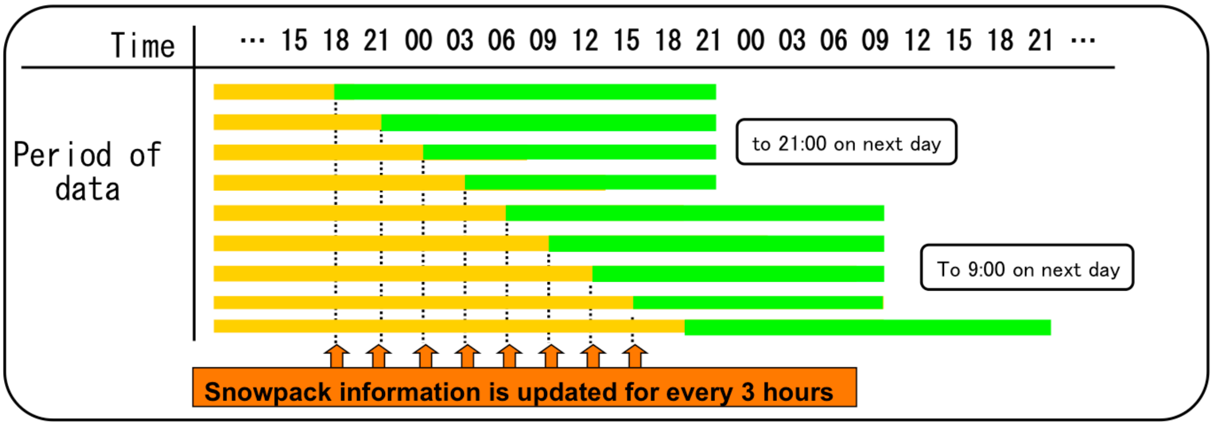

Figure 1 Schedule to update snowpack information. Yellow: using observed data; green: using predicted data. Meteorological prediction data is updated for every 12 hours.

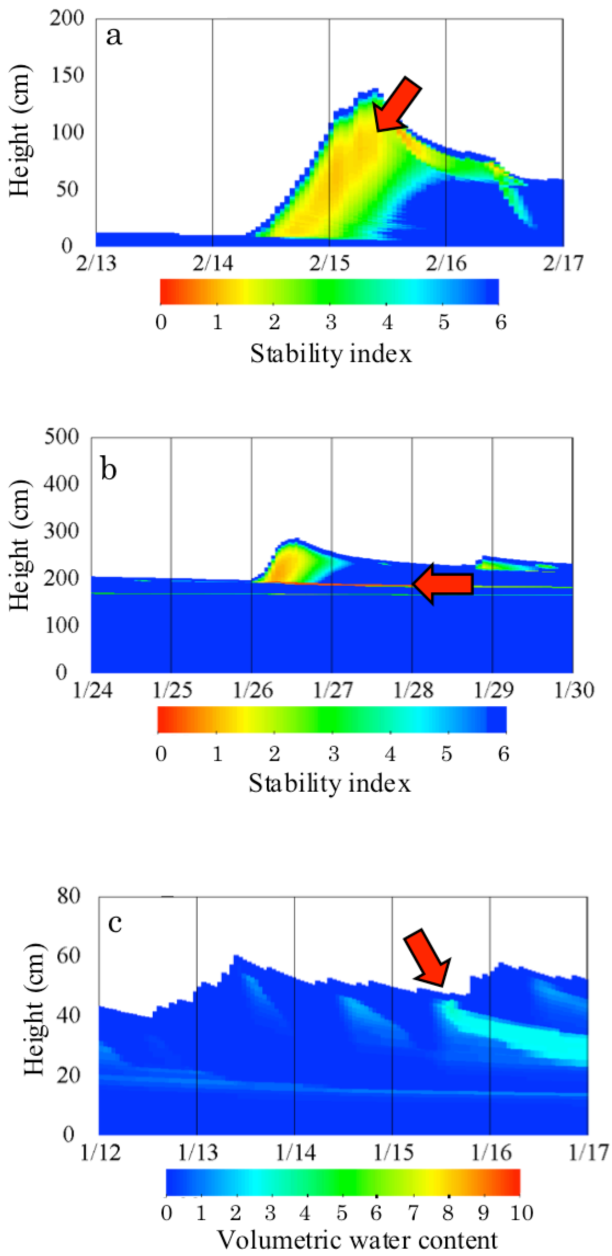

Figure 2 Examples of low stability snowpacks at risk of avalanche under; a: heavy snowfall, b: snowfall with a weak layer, and c: wet snow with liquid water infiltration.

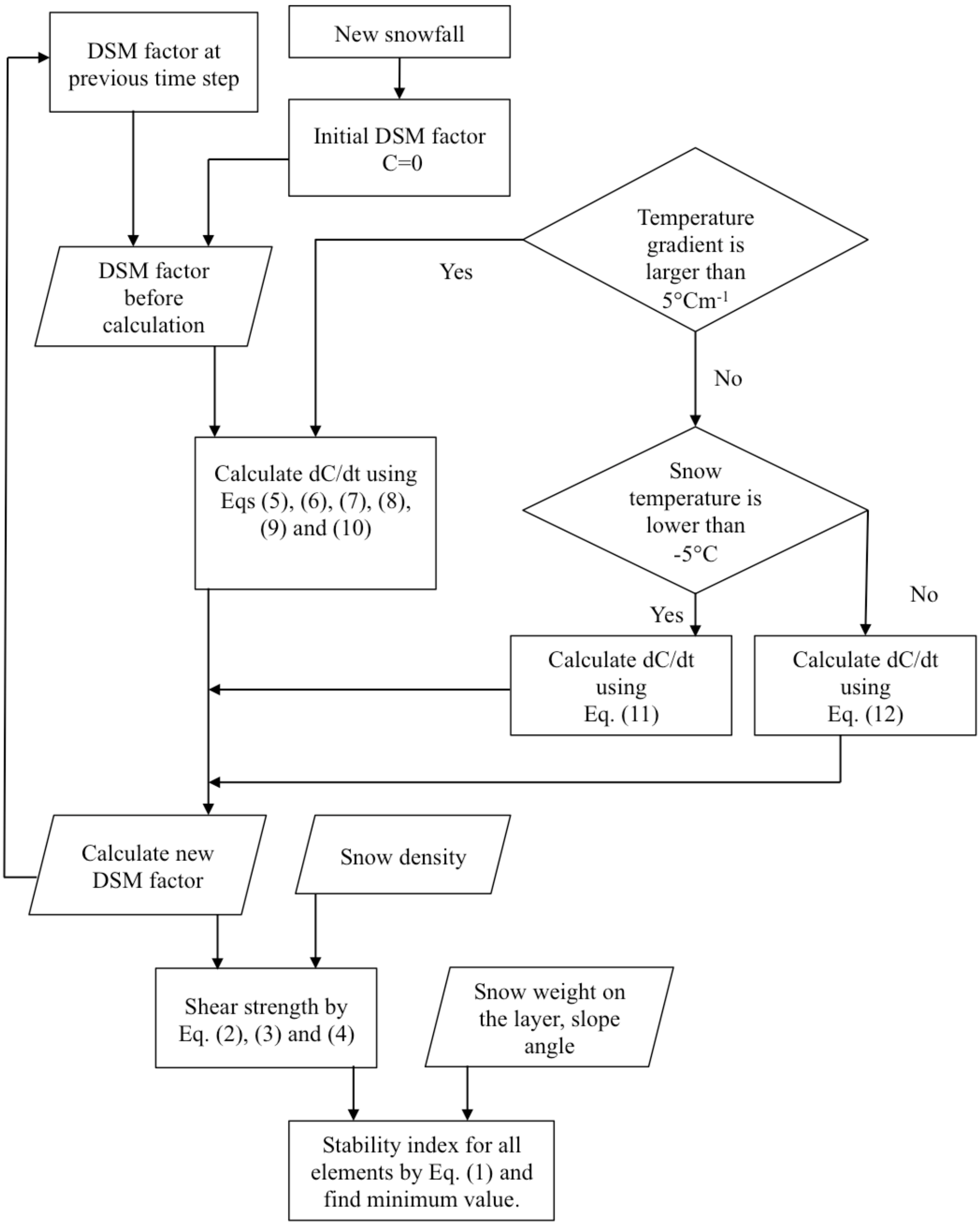

Figure 3 Flow chart for simulation of the natural stability index using DSM factor to estimate avalanche risk. See Table 3 for explanation of symbols.

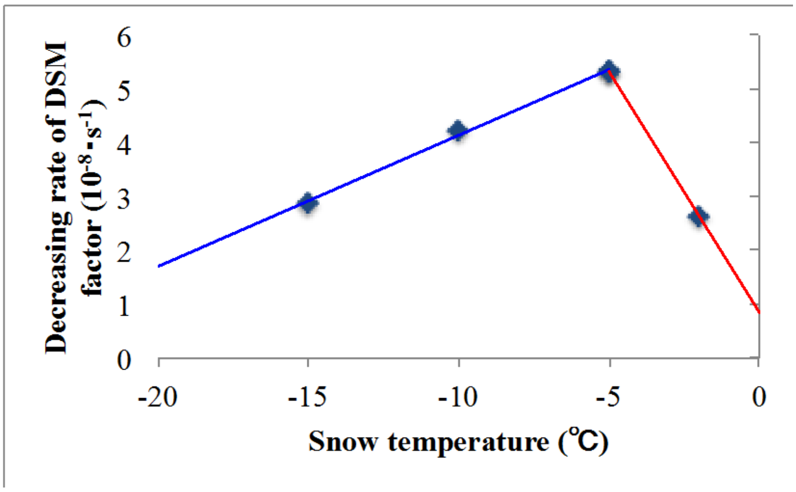

Figure 4 Rate of reduction of the dry snow metamorphism (DSM) factor during equi-temperature metamorphism depending on snow temperature (Hirashima *et al.*, 2011; Hirashima and Abe, 2012).

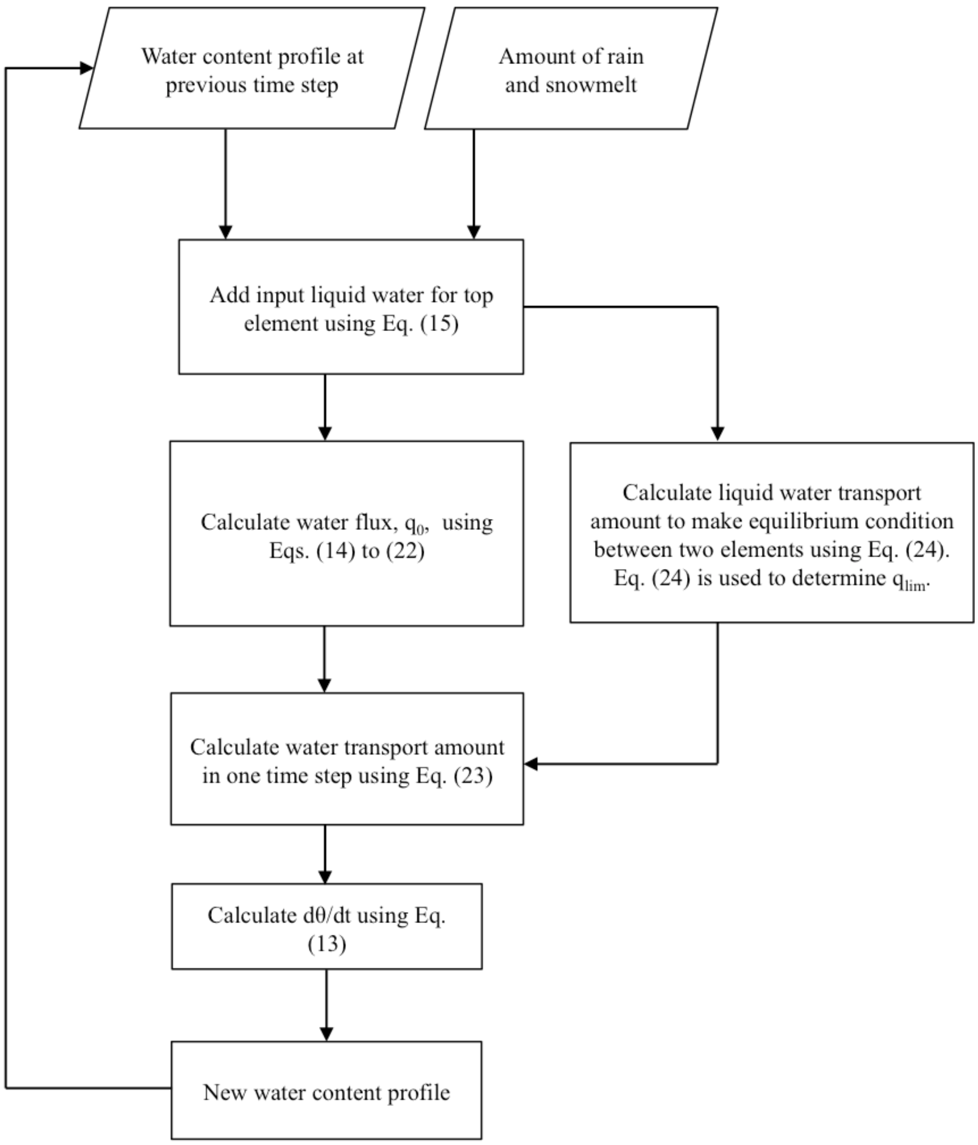

Figure 5 Flow chart for simulation of liquid water infiltration into the snowpack. See Table 3 for explanation of symbols.

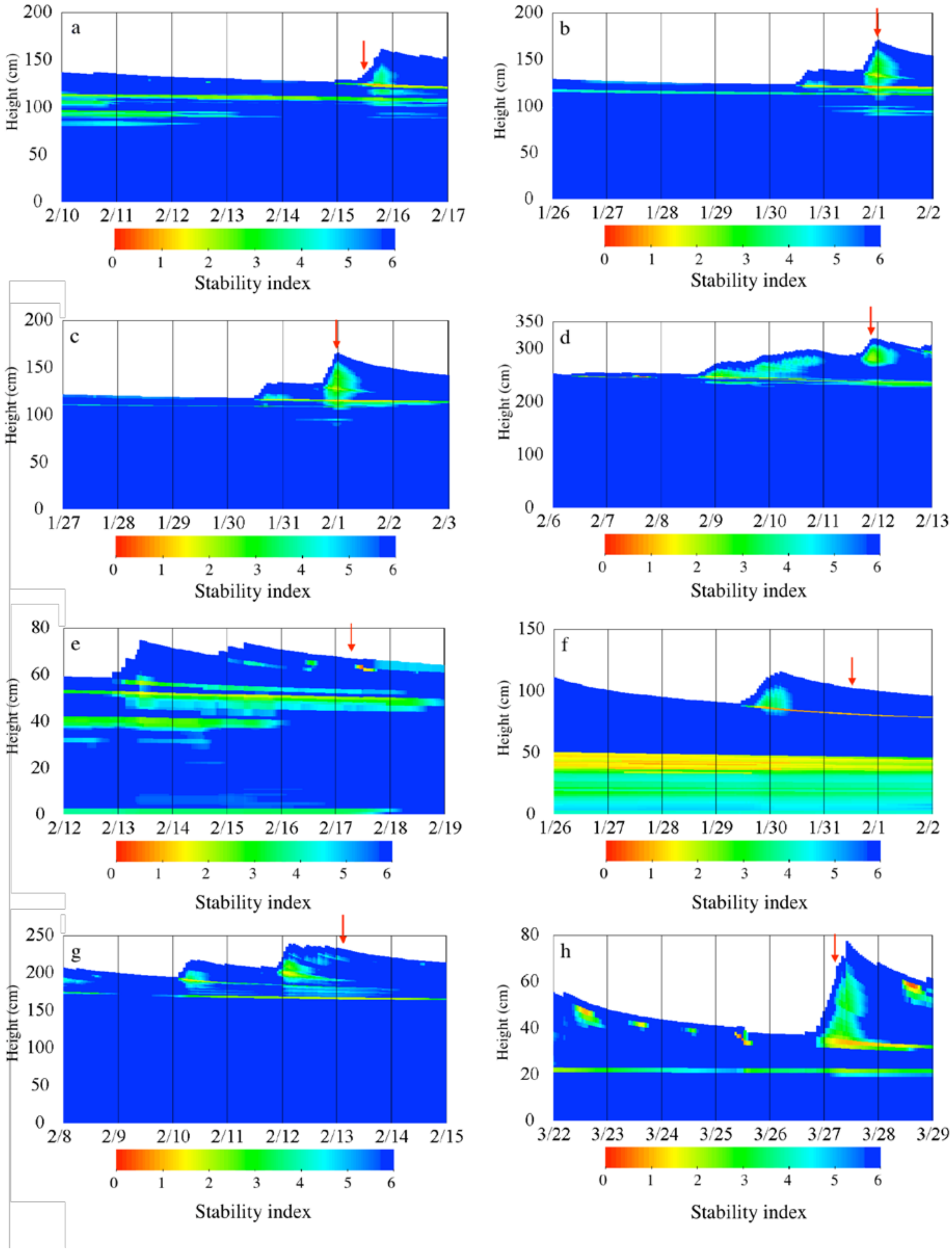

513

514 Figure 6 Simulated natural stability indices for surface avalanches in 2014–2017. Red arrows

515 show the timings of avalanche release. See Table 4 for details of the avalanches.